Encapsulation, characterization and catalytic properties of uranyl ions in mesoporous molecular sieves

K. Vidya [a], S.E. Dapurkar [a], P. Selvam [a,*], S.K. Badamali [b],
D. Kumar [b], N.M. Gupta [b]

[a] *Department of Chemistry, Indian Institute of Technology-Bombay, Powai, Mumbai 400076, India*
[b] *Applied Chemistry Division, Bhabha Atomic Research Center, Trombay, Mumbai 400085, India*

Abstract

Occlusion of uranyl ions (UO_2^{2+}) in the pore channels of mesoporous MCM-41 and MCM-48 molecular sieves was accomplished using direct template ion-exchange method, and the samples were characterized by X-ray diffraction (XRD), Fourier transform infrared spectroscopy (FT-IR), diffuse reflectance ultraviolet–visible spectroscopy (DRUV–VIS), and fluorescence spectroscopy. A shift in U=O stretching IR band ($\Delta \nu = -34\,cm^{-1}$), and the appearance of broad and diffused bands in the fluorescence spectra (480–620 nm) of the UO_2^{2+}-exchanged samples indicate a definite electronic interaction of UO_2^{2+} species with the silicate ($\equiv Si–O^-$) surface. This inference is corroborated by DRUV–VIS results. Calcination in air/N_2 at 823 K resulted in the formation of well-dispersed α-U_3O_8/α-U_3O_7 moieties, accompanied by a marginal decrease in the concentration of UO_2^{2+} groups. The binding of UO_2^{2+} species to mesoporous materials framework remained intact even after calcination. The molecular sieves loaded with uranium oxide species showed appreciable activity, both for the oxidation of CO and for adsorption/decomposition of CH_3OH. © 2002 Elsevier Science B.V. All rights reserved.

Keywords: Uranyl species; Mesoporous materials; Catalytic activity; MCM-41; MCM-48

1. Introduction

Mesoporous molecular sieves have received wide attention because of their diversified applications as shape selective catalysts, adsorbents, ion-exchangers and also in removal of heavy metal ions, radionuclides and organics from effluents [1–3]. The well-defined (tunable) pore sizes and the large pore openings of these molecular sieves render them unique host materials for occlusion/anchoring of large molecules or that of reactive metal complexes in their channels.

The incorporation of specific functional groups onto the walls of the channels in these molecular sieves thus serves as an important step in heterogenizing the homogeneous catalyst systems. In consideration that uranium (i.e. uranyl ions or uranium oxides) may serve as promising oxidizing catalyst owing to its variable valence states vis-à-vis vacant f-orbitals [4,5], we have attempted the encapsulation of uranyl species (UO_2^{2+}) in the mesopores of hexagonal MCM-41 and cubic MCM-48 molecular sieves. The emphasis was to achieve a well-dispersed catalyst system for oxidation reactions. Earlier studies in this direction concern dispersion of uranium oxides over dense oxide supports such as Al_2O_3, TiO_2, SiO_2, MgO, etc. [6].

* Corresponding author. Tel.: +91-22-576-7155;
fax: +91-22-572-3480/576-7152.
E-mail address: selvam@iitb.ac.in (P. Selvam).

In the present investigation, we adopted a direct template ion-exchange method [7] for the entrapment of uranyl species (UO_2^{2+}) in the mesopores of MCM-41 and MCM-48 silicates. The samples in the as-synthesized, as-exchanged and corresponding calcined forms were characterized by various techniques such as X-ray diffraction (XRD), induced coupled plasma–atomic emission spectroscopy (ICP–AES), Fourier transform infrared spectroscopy (FT-IR), diffuse reflectance ultraviolet–visible spectroscopy (DRUV–VIS), and fluorescence spectroscopy. The catalytic performance of these materials was evaluated for model reactions, viz. oxidation of CO and adsorption/decomposition of CH_3OH over a temperature range 373–773 K.

2. Experimental

2.1. Synthesis of MCM-41 and MCM-48

The mesoporous MCM-41 and MCM-48 silicates were synthesized hydrothermally as per the procedure described elsewhere [8,9]. The typical gel (molar) composition was $10SiO_2:1.35(CTA)_2O:0.75(TMA)_2O:1.3Na_2O:680H_2O$ for MCM-41, and $10SiO_2:3(CTA)_2O:2.5Na_2O:600H_2O$ for MCM-48. The gels were crystallized in Teflon-lined stainless steel autoclaves at 373 K for 1 and 3 days for MCM-41 and MCM-48, respectively. The solid products obtained were washed with distilled water several times, filtered, and dried at 353 K, and were designated as as-synthesized samples.

2.2. Preparation of UO_2^{2+}-exchanged MCM-41 and MCM-48

The entrapment of UO_2^{2+}-ions in the mesoporous materials was carried out by contacting 1 g sample of as-synthesized MCM-41 or MCM-48 with 80 ml of aqueous uranyl acetate solution (0.035 molar) at a pH of 4, under constant stirring at 323 K. Different loading of uranium were achieved by varying contact time, 12–54 h. A saturation loading of UO_2^{2+}-ion was reached in around 20 h time using both as-synthesized MCM-41 and MCM-48. The latter, however, showed a higher saturation uranium uptake ($\sim$53 wt.% of uranium as metal) compared to MCM-41 (43 wt.%). The

details can be seen elsewhere [10]. For the experiments carried out in the present study, the samples with the saturation uranium loading were utilized. The solid mass after decantation was washed repeatedly, followed by filtration and drying at 353 K for 5 h. The UO_2^{2+}-exchanged samples were calcined first in N_2 for 1–2 h and then for 6 h in air at 823 K. The effect of calcination in N_2 on the oxidation state of occluded UO_2^{2+} species was also evaluated.

2.3. Characterization

Powder XRD patterns of the ion exchanged and calcined samples were recorded in 2θ region of 1–10° on Rigaku diffractometer using a nickel filtered Cu Kα radiation. The scan speed and step size was 0.2° min^{-1} and 0.02°, respectively. The diffraction patterns were also recorded in higher 2θ region (10–60°) in order to identify the bulk uranium phases. FT-IR spectra in mid IR region were recorded on a JASCO model-610 spectrometer at a resolution of 4 cm^{-1} and using 6 wt.% of a sample in a compressed KBr pellet. For each spectrum 100 scans were co-added. UV-fluorescence spectra were obtained on a Hitachi, F-4500 fluorescence spectrophotometer, using a monochromated 310 nm radiation for excitation and a UV-35 filter to cut off this radiation in emission spectrum. DRUV–VIS spectra of uranium-containing samples were recorded on a Shimadzu UV-260 spectrophotometer.

The catalytic activity was determined in pulse mode using a tubular quartz reactor (8 mm o.d.) in a temperature range of 473–773 K and at ambient pressure. A catalyst charge of ca. 150 mg was loaded in the reactor in between quartz wool plugs. While the catalyst was maintained under He flow (30 ml min^{-1}), successive pulses (500 μl each) of feed mixture (CO:O_2 = 2:1) were introduced at a desired temperature. In the case of experiments involving methanol decomposition, reactant feed mixture was 9 vol.% of methanol vapor in argon. The time interval between two pulses was around 30 min. Prior to the run, the catalyst was activated at 623 K under He and O_2 flow. A Chemito model-8510 gas chromatograph, equipped with thermal conductivity detector and Porapak-QS/Sperocarb column, was employed for on-line analysis of the reactant and product species.

3. Results and discussion

3.1. XRD studies

XRD patterns of both as-synthesized and UO_2^{2+}-exchanged MCM-41 showed typical reflections 100, 110, 200, and 210 in the range 2–5°, characteristic of MCM-41 [8]. Similarly, the XRD pattern of as-synthesized MCM-48 and corresponding UO_2^{2+}-exchanged sample showed two major reflections at 211 and 220, in addition to six minor reflections 321, 400, 420, 332, 422, and 431 in the range 3.5–5°, typical of MCM-48 [8]. However, a decrease in the intensity of the reflections was observed in case of UO_2^{2+}-exchanged samples [10] indicating a partial loss of crystallinity. This could be attributed to the partial hydrolysis of $\equiv$Si–O–Si$\equiv$ linkages of the mesoporous silicate network during the exchange process. No diffraction reflections due to uranium (bulk oxide) phases were detected in the as-exchanged samples. Upon calcination, weak reflections at $d = 4.15, 3.39, 2.62, 2.07, 1.96$ and 1.75 Å were observed, which can be indexed for α-U_3O_8 (JCPDS Card No.24-1172). The formation of this uranium oxide phase may be attributed to the dehydroxylation of the uranyl oligomers, followed by oxidation. It may be noted that in addition to UO_2^{2+}-ions, abundance of other hydrolyzed species/oligomers such as $(UO_2)_2(OH)_2^{2+}$ and $(UO_2)_3(OH)_5^+$ in uranyl solution has been reported under the concentration and the pH conditions used in the present study [11,12]. The samples calcined exclusively in N_2 atmosphere indicated the formation of α-U_3O_7 ($d = 3.43, 3.13, 2.88, 2.71, 1.92, 1.63$ and 1.54 Å; JCPDS Card No.15-4).

3.2. FT-IR studies

Typical FT-IR spectra of unloaded, UO_2^{2+}-exchanged, and UO_2^{2+}-exchanged and calcined MCM-48 are shown in Fig. 1. Corresponding data for MCM-41 are shown in Fig. 2. In the IR spectra, the absorbance values of the selected bands are reported in parentheses for a comparative evaluation of their intensities. The IR bands at $\sim$2922 and 2852 cm^{-1} are typical of CTA$^+$(ν_{C-H}) group. The major bands appearing between 1230 and 459 cm^{-1} are attributed to various stretching ($\nu_{Si-O-Si}$) and bending ($\delta_{Si-O-Si}$) frequencies of $\equiv$Si–O–Si$\equiv$ linkages. The band at
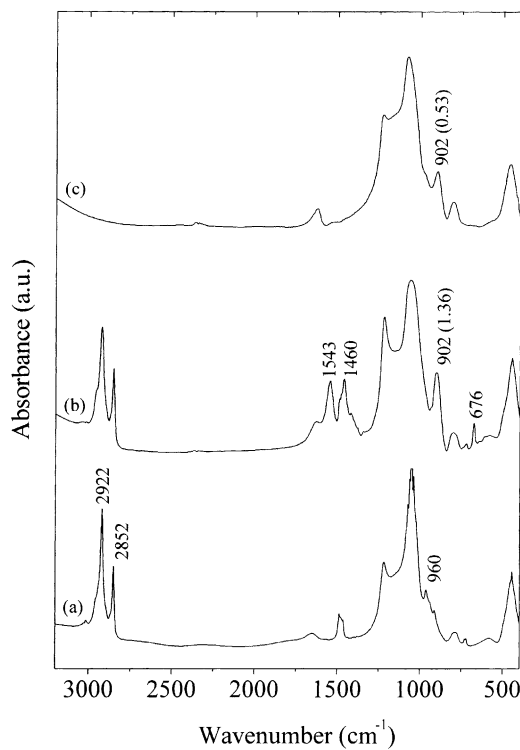

Fig. 1. FT-IR spectra of MCM-48: (a) as-synthesized, (b) UO_2^{2+}-exchanged and (c) UO_2^{2+}-exchanged and calcined. The values in parenthesis indicate the absorbance values.

960 cm^{-1} is due to defect sites ($\equiv$Si–O$^-$$\cdots$X$^+$, where X$^+$: Na$^+$, CTA$^+$ or H$^+$). All these bands are characteristic features of the MCM-41 and MCM-48 silicate framework [13]. An additional IR band appearing at $\sim$902 cm^{-1} in the UO_2^{2+}-exchanged samples of MCM-48 or MCM-41 (Figs. 1b and 2b) may be attributed to $\nu_{U=O}$ stretching vibrations of uranyl species [14]. The bands appearing at 1543, 1460 cm^{-1} (ν_{COO}) and 676 cm^{-1} (δ_{OCO}) are characteristic of the acetate ions [15].

As reported widely [16], the UO_2^{2+} groups are linear, and in uranyl acetate they exhibit a strong absorption band at $\sim$930 cm^{-1} due to asymmetric U=O stretch; the corresponding symmetric vibration expected at $\sim$856 cm^{-1} is observed only in very thick samples. It is well documented that the U=O stretching frequency in a uranyl compound changes with the ligand and a relationship exists between this frequency and the U=O bond distance [14]. A red shift
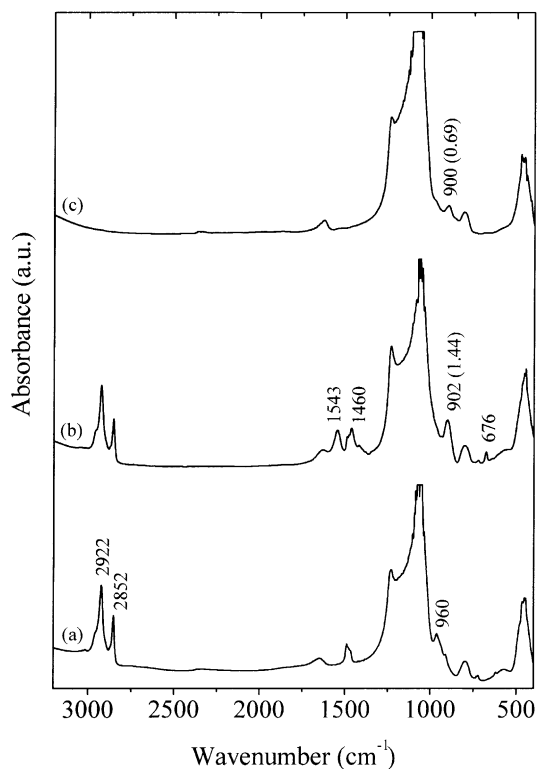
Fig. 2. FT-IR spectra of MCM-41: (a) as-synthesized, (b) UO_2^{2+}-exchanged and (c) UO_2^{2+}-exchanged and calcined.

Fig. 3. Fluorescence spectra of MCM-48: (a) UO_2^{2+}-exchanged and (b) UO_2^{2+}-exchanged and calcined. Excitation wavelength: 310 nm.

of $\sim$30 cm^{-1} in this band, as seen in Figs. 1b and 2b, thus, indicates a perturbation of adsorbed uranyl ions, arising from their bonding (through oxygen of uranyl group) with the mesoporous framework, hence weakening the U=O bond. On calcination, these bands are seen in the nearly at the same frequencies when the acetate groups are removed completely (Figs. 1c and 2c). The intensity of 902 cm^{-1} band, however, decreases marginally on calcination (Figs. 1c and 2c), indicating that a part of UO_2^{2+} groups transform to other uranium oxides during the calcination process, as is evident from XRD data. From the relative intensities of ν_{C-H} at 2922 cm^{-1} and $\nu_{U=O}$ at 906 cm^{-1}, as seen in an earlier study [10], it is evident that the attachment of UO_2^{2+}-ions is accompanied with the progressive removal of CTA$^+$-ions. It may thus be inferred that the anchoring of the uranyl group occurs via direct replacement of template ions, as is brought out in [10] in detail.
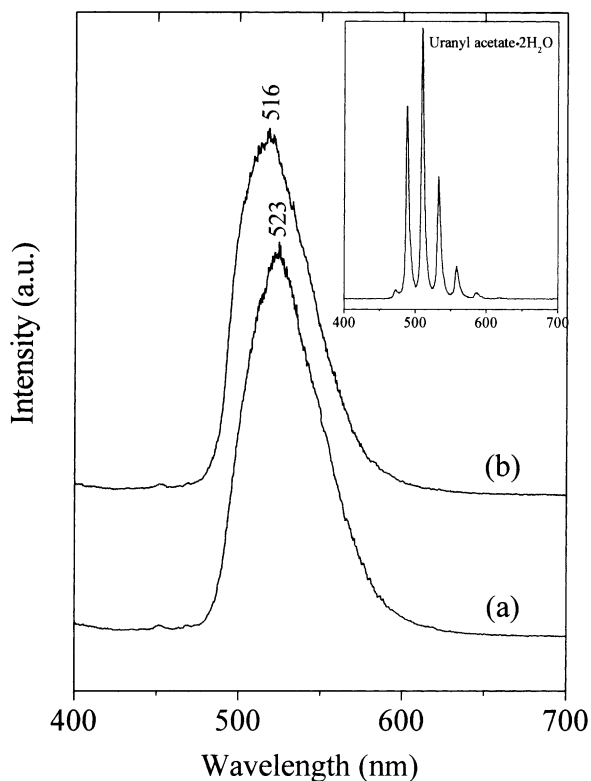
3.3. UV-fluorescence studies

The UV-fluorescence study (Fig. 3) provides important information regarding the form in which uranium is present in the mesopores. Curves (a) and (b) present the representative fluorescence spectra of UO_2^{2+}-exchanged MCM-48 before and after calcination, respectively. For a comparison, the fluorescence spectrum of uranyl acetate is shown in inset. It gives rise to several well defined and sharp emission bands in the 470–590 nm range, which are assigned to transitions between vibrational level of first excited electronic state ($\nu' = 0$) to vibrational levels of ground electronic state ($\nu'' = 0$–5) of uranyl ions [17]. On the other hand, UO_2^{2+}-exchanged MCM-48 shows considerably broad and overlapping emission bands between 484 and 620 nm (curve). Apart from that, all the band positions are shifted to higher wavelength, which is an indication of weakening of the uranyl

(U=O) linkages. This can be envisaged to happen as a result of an interaction of UO_2^{2+}-ions with the silicate ($\equiv$Si–O$^-$ groups) matrix, as discussed above. A decrease in the intensity of the emission bands after calcination (Fig. 3b) is consistent with our IR data suggesting the transformation of some of the UO_2^{2+} species giving rise to non-fluorescent uranium oxides, the presence of which is also revealed by XRD data. A comparison between Fig. 3a and b shows a small but reproducible blue shifted ($\Delta\lambda = -7$ nm) in the wavelength of the emitted radiation after calcination of the as-exchanged sample. This could be tentatively ascribed to their less constrained environment after the removal of template ions. Further, as in case of IR result, similar fluorescence behavior was observed in the UO_2^{2+}-exchanged MCM-41 samples.

3.4. DRUV–VIS studies

The DRUV–VIS spectra of UO_2^{2+}-exchanged MCM-41 and MCM-48 are shown in curves a and c of Fig. 4, respectively. For a comparison, the spectrum of uranyl acetate is included (curve e), which shows the characteristic structure due to electron-vibration interaction, typical of UO_2^{2+} moiety [18]. The distinct structure of the uranyl spectrum with sharp bands is ascribed to definite transitions from electronic levels coupled to O=U=O vibrations [18]. The comparison of spectra of the UO_2^{2+}-exchanged sample with that of uranyl acetate reveals that the UO_2^{2+}-exchanged samples also exist in the hexavalent state in the form of UO_2^{2+} species. It is also observed that the spectra of UO_2^{2+}-exchanged samples may be attributed to the bonding of $\equiv$Si–O$^-$ units to linear O=U=O molecules in the equatorial plane forming a uranate type of local structure, similar to an observation reported elsewhere [18]. Fig. 4b and d show the DRUV–VIS spectra of UO_2^{2+}-exchanged and calcined MCM-41 and MCM-48 samples. It is observed that the maximum appearing at $\sim$430 nm in UO_2^{2+}-exchanged MCM-41 shifts to a shorter wavelength in the corresponding calcined sample ($\sim$421 nm). Similarly, a shift from $\sim$430 to $\sim$424 nm is observed for the UO_2^{2+}-exchanged MCM-48. It has been generally agreed that the nature of blue shift of the visible and the near infrared bands may be taken as a measure of the metal–ligand covalent bonding [19]. This hypsochromic shift seen in Fig. 4b and d could, therefore,
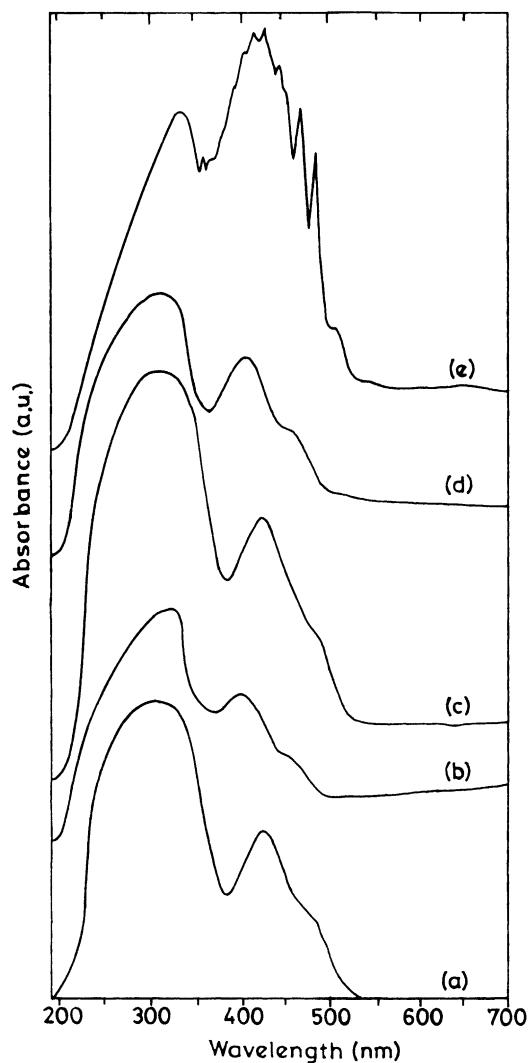

Fig. 4. DRUV–VIS spectra: (a) UO_2^{2+}-exchanged MCM-41, (b) UO_2^{2+}-exchanged and calcined MCM-41, (c) UO_2^{2+}-exchanged MCM-48, (d) UO_2^{2+}-exchanged and calcined MCM-48 and (e) uranyl acetate dihydrate.

be taken as a reflection on the stability of the UO_2^{2+} species in the mesoporous matrix due to a strong interaction between UO_2^{2+} and the $\equiv$Si–O$^-$ sites, as mentioned above.

3.5. Catalyst activity studies

In order to evaluate catalytic activity of the uranium-containing mesoporous molecular sieves,
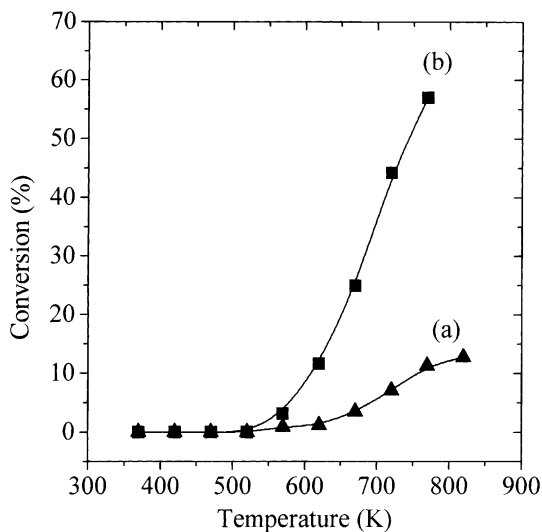
Fig. 5. Catalytic oxidation of CO over (a) MCM-48 and (b) UO_2^{2+}-exchanged and calcined MCM-48.

Fig. 6. Reaction products formed on exposure of methanol pulses over UO_2^{2+}-exchanged and calcined MCM-48 (a) CO_2, (b) CO and (c) CH_4.

two model reactions, viz. oxidation of CO and adsorption/decomposition of CH_3OH were chosen for study over the temperature range of 373–773 K. Typical results obtained for uranium-containing (53 wt.%) MCM-48 are presented here in brief.

3.5.1. CO oxidation

The uranium-containing MCM-48 showed considerably high catalytic activity compared to host MCM-48, as shown in data of Fig. 5. Around 60% of CO dosed in a pulse over uranium-containing MCM-48 converted to CO_2 at a temperature of 770 K (curve b), the corresponding yield over host MCM-48 being less than 10% (curve a). Also the activity onset temperature is relatively low in the uranium-containing molecular sieve. This oxidative activity can be attributed to the definite role of UO_2^{2+}-ions and/or oxides for the conversion of CO to CO_2, in agreement with [20].

3.5.2. Methanol adsorption/decomposition

A higher amount of methanol was adsorbed/reacted over uranium-containing MCM-48 compared to the host matrix. While no unreacted methanol was eluted when successive 6–7 pulses of methanol (14.8 μmol each) were dosed over uranium loaded sample at temperatures in range 470–770 K, about 25, 11, and
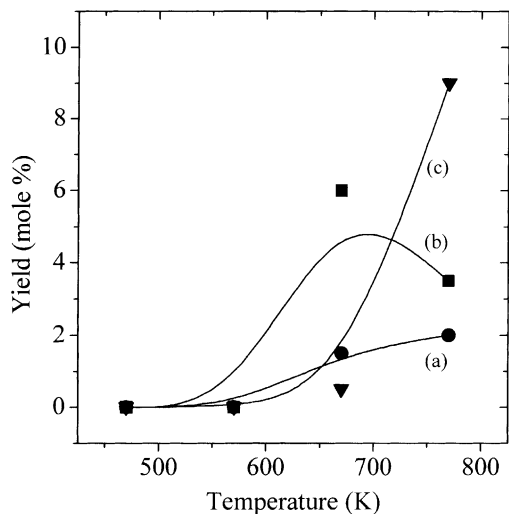
5 vol.% of methanol was eluted from each of these pulses, when introduced over MCM-48 at temperatures of 470, 570, and 770 K, respectively. The reaction products were also different. Thus, while reaction over MCM-48 predominantly gave rise to formation of dimethyl ether ($\sim$1.7 mol%) at temperatures above 670 K, the reaction products over uranium-containing MCM-48 were CO, CO_2 and CH_4. The product distribution for reaction of CH_3OH over uranium-containing MCM-48 as a function of temperature is shown in Fig. 6. The difference in catalytic behavior of two samples can be attributed to the difference in the catalyst nature. In case of MCM-48, due to the presence of weakly acidic $\equiv$Si–OH groups, the products obtained are catalyzed by an acid pathway. On the contrary, in uranium-containing MCM-48, the reaction is catalyzed by an oxidative route, yielding CO, CO_2, and CH_4 [21].

4. Conclusions

In the present investigation, the successful entrapment of UO_2^{2+}-ions within the mesopores of MCM-41 and MCM-48 is demonstrated. MCM-48 was found to be trapping higher amount of UO_2^{2+}-ions

than MCM-41. Under the experimental conditions, it was observed that both MCM-41 and MCM-48 suffer a partial loss in crystallinity, even though the structure does not collapse. Both FT-IR and fluorescence studies indicated the binding of UO_2^{2+}-ions onto the silicate surface, possibly via an interaction between $\equiv Si–O^-$ and the UO_2^{2+}-ions. Upon calcination, UO_2^{2+} moieties are partly converted to uranium oxide species (α-U_3O_7/α-U_3O_8), which are dispersed within the mesoporous matrix. Further, the results of catalytic oxidation of CO and adsorption/decomposition of CH_3OH indicate that the entrapped UO_2^{2+}-ions and/or oxides may serve as potential candidates for the selective oxidation reactions. Further study is in progress to corroborate these claims.

Acknowledgements

References

[1] A. Stein, B.J. Melde, R.C. Schroden, Adv. Mater. 12 (2000) 1403.

[2] K. Moller, T. Bein, Chem. Mater. 10 (1998) 2950.

[3] A. Corma, Chem. Rev. 97 (1997) 2373.

[4] C.A. Colmenares, Prog. Solid State Chem. 15 (1984) 257.

[5] A. Collette, V. Deremince-Mathien, Z. Gabelica, J.B. Nagy, E.G. Derouane, J.J. Verbist, J. Chem. Soc., Faraday Trans. 83 (1987) 1263.

[6] H. Collette, S. Maroie, J. Riga, J.J. Verbist, Z. Gabelica, J.B. Nagy, E.G. Derouane, J. Catal. 98 (1986) 326.

[7] S. Dai, Y. Shin, Y. Ju, M.C. Burleigh, J.-S. Lin, C.E. Barnes, Z. Xue, Adv. Mater. 11 (1999) 1226.

[8] J.S. Beck, J.C. Vartuli, W.J. Roth, M.E. Leonowicz, K.D. Schrnidtt, C.T.-W. Chu, D.H. Olson, E.W. Sheppard, S.B. McCullen, J.B. Higgins, J.L. Schienker, J. Am. Chem. Soc. 114 (1992) 1083;
P. Selvam, S.K. Bhatia, C. Sonwane, Ind. Eng. Chem. Res. 40 (2001) 3237.

[9] S.E. Dapurkar, S.K. Badamali, P. Selvam, Catal. Today 68 (2001) 63.

[10] K. Vidya, S.E. Dapurkar, P. Selvam, S.K. Badamali, N.M. Gupta, Microporous Mesoporous Mater. (2001), in press.

[11] C.H. Ho, D.C. Doern, Canada J. Chem. 63 (1987) 1100, and references cited therein.

[12] R. Amadelli, A. Maldotti, S. Sostero, V. Carassiti, J. Chem. Soc., Faraday Trans. 87 (1991) 3267.

[13] C.-Y. Chen, H.-X. Li, M.E. Davis, Micropor. Mater. 2 (1993) 17.

[14] K. Nakamoto, Infrared and Raman Spectra of Inorganic and Coordination Compounds, Wiley, New York, 1978.

[15] S.V. Ribnikar, M.S. Trtica, J. Serb. Chem. Soc. 63 (1998) 149.

[16] E. Rabinowitch, R.L. Belford, Spectroscopy and Photochemistry of Uranium Compounds, Pergamon Press, Oxford, 1964.

[17] S.G. Schulman, Molecular Luminescence Spectroscopy Methods and Applications (Part 1), Wiley, New York, 1985.

[18] L. Sacconi, G.J. Giannoni, Chem. Soc. (1954) 2368.

[19] C.K. Jorgensen, Prog. Inorg. Chem. 4 (1962) 73.

[20] F. Nozaki, I. Inami, Bull. Chem. Soc. Jpn. 45 (1972) 3473.

[21] J.M. Tatibouet, Appl. Catal. 148 (1997) 213.